Penerbit Akademia Baru

Journal of Advanced Research in Applied Mechanics
ISSN (online): 2289-7895 | Vol. 24, No. 1. Pages 1-21, 2016

Mixed Convective Nanofluids Flow in a Channel having Forward-Facing Step with Baffle

H.A. Mohammed[1], *O. A. Alawi*[2], *N. A. Che Sidik*[*,2]

[1]Technical College of Engineering, Duhok Polytechnic University (DPU), 61 Zakho Road, 1006 Mazi Qr, Duhok-Kurdistan Region, Iraq
[2]Faculty of Mechanical Engineering, Universiti Teknologi Malaysia, 81310 Skudai Johor, Malaysia
[*]*azwadi@mail.fkm.utm.my*

Abstract – *Two-dimensional laminar and turbulent mixed convection flows using nanofluids over forward facing step in a heated rectangular duct having a baffle mounted on its wall are numerically simulated. The continuity, momentum and energy equations are solved using finite volume method (FVM) and the SIMPLE algorithm scheme is applied to examine the effects of the baffle on flow and heat transfer characteristics. The bottom wall of the duct is being heated with a constant heat flux, while other walls are being thermally insulated. In this study, several parameters such as different types of nanoparticles (Al_2O_3, CuO, SiO_2 and ZnO), different volume fractions in the range of 1% to 4%, different nanoparticles diameter in the range of 25 to 80 nm were used. The Reynolds number of laminar flow was in the range of $100 \leq Re \leq 500$, while for turbulent flow it was in the range of $7500 \leq Re \leq 15000$. Effects of baffle distances in the range of $\infty \leq D \leq 4$, baffle widths in the range of $0.01 \leq w_b \leq 0.04$, baffle heights in the range of $0.005 \leq h_b \leq 0.015$ were studied. Baffle locations at the top wall and at bottom wall of the duct, and the number of baffles are from 1 to 3 were also examined. The numerical results indicate that the nanofluid with SiO_2 has the highest Nusselt number compared with other nanofluids types. The Nusselt number increases as the volume fraction of nanoparticles and the Reynolds number increase, while it decreases as the nanoparticles diameter increases. Effects of baffle distances baffle heights, and baffle locations on fluid flow and heat transfer characteristics are significant, while effects of baffle widths and baffle numbers are slightly insignificant.*

Keywords: Mixed convection, forward facing step, Nanofluids, Channel flow, Baffle installation

1.0 INTRODUCTION

In engineering practice, most of the flow fields are generally in turbulent regime. However, in many of these, flow separation and reattachment occurs depending on flow velocity and physical model. Forward and backward facing step flow, which can be found in cooling of electronic devices, open channels, combustion chambers and building aerodynamics, are good examples for this kind of separating flows. Forward facing step (FFS) is more complicated than backward facing step in which only one separated flow region occurs behind the step. However,

Journal of Advanced Research in Applied Mechanics
ISSN (online): 2289-7895 | Vol. 24, No. 1. Pages 1-21, 2016

one or more separating region can be found in FFS depending on the thickness of boundary layer and magnitude of flow velocity as indicated in the literature [1].
An innovative technique for improving heat transfer by using ultra fine solid particles in the fluids has been used extensively during the last decade. The particles are different from conventional particles (millimeter or micro-scale) in that they keep suspended in the fluid and no sedimentation occurs which causes no increase in pressure drop in the flow field. Therefore, it is very useful to enhance heat transfer in separated regions by using nanofluids. Such enhancement is accomplished by increasing the value of convective heat transfer coefficient (or Nusselt number) in separated flows [2-5].

Abu-Mulaweh et al. [6] made an experiment and theoretical analysis for laminar mixed convection flow over horizontal FFS geometry. They used Laser–Doppler Velocimeter and cold wire anemometer for measurements. In another study by Abu-Mulaweh et al. [7], they studied the laminar natural convection problem for vertical FFS both numerically and experimentally. Wilhelm et al. [8] performed a computational study to show 2-D to 3-D transition in FFS flow at Re = 330. An experimental and numerical analysis was performed to investigate separation on FFS flow by Stuer [9]. He used hydrogen bubble visualization technique. He indicated that the 2-D results but 3-D flow behavior starts beyond the critical Re number according to his experimental results. Abe et al. [10] proposed the new turbulence model which is modified from the latest low-Re number $k-\varepsilon$ model and then they applied it for fluid flow and heat transfer in separating and reattaching flows. Ando and Shakouchi [11] tried to control flow over FFS and abrupt contraction pipe geometry. They inserted a small obstacle before the step and then they reduced the drag. Ito and Ravindran [12] applied the reduced order method to solve and control viscous incompressible flow control for different geometries. They applied surface movement on a part of the solid wall of the geometry, thus, drag reduced is obtained.

The heat flux in thermal devices has become more and vast due to the increasing requirements of compactness for the relative systems. It should be important to seek ways to effectively augment the heat transfer characteristics of backward-facing step flow in channels. Among important studies Tsay et al. [13] examined the influence of baffle vertically mounted onto the channel wall on the convective behaviors of backward-facing step flow. Comparing the results of cases with and without baffle, the maximum augmentation on the average Nusselt number is about 190% for the heating step and 150% for the heating section of the bottom plate. Berner et al. [14, 15] obtained experimental result of mean velocity and turbulent distributions in flow around 12 segmented baffles. After about two baffles, the profiles of vertical mean velocity and fluctuations along the horizontal center plan become periodic. Experimental investigation of the turbulent flow and heat transfer characteristics inside the periodic cell formed between segmented baffles staggered in a rectangular duct was studied by Habib et al. [16] Numerical prediction of the flow and heat transfer in channel with staggered fins were investigated by Webb and Ramadhyani [17], Kelkar and Patankar [18], and Habib et al. [19].

Very few number of research work were conducted numerically and experimentally by Dutta and Dutta [20], and Yang and Huang [21] to capture more detail of the fluid flow pattern and heat transfer phenomena in the channel with perforated baffle. Three-dimensional laminar convection flow adjacent to backward-facing step in a heated rectangular duct with a baffle mounted on the upper wall was numerically simulated by Nie et al. [22].

There are rather limited articles that have been reported in the literature on the convective heat transfer in nanofluids. It should be noted, however, that the vast majority of the studies of a

Penerbit Akademia Baru
Journal of Advanced Research in Applied Mechanics
ISSN (online): 2289-7895 | Vol. 24, No. 1. Pages 1-21, 2016

backward-facing step that are reported in the open literature involved "regular" fluids (i.e., not nanofluids). Very few studies that involve nanofluids in backward-facing step geometry have been reported in the past. The first numerical study to investigate the flow and heat transfer over a backward-facing step using nanofluids is by Abu-Nada [23]. The Reynolds number and nanoparticles volume fraction used were in the range of $200 \leq Re \leq 600$ and $0 \leq \varphi \leq 0.2$, respectively, for five types of nanoparticles which are Cu, Ag, Al_2O_3, CuO, and TiO_2. He reported that the high Nusselt number inside the recirculation zone mainly depended on the thermophysical properties of the nanoparticles and it is independent of Reynolds number. Numerical analysis of the forced and mixed convection (buoyancy-assisting flow condition) over a vertical and horizontal backward facing step in a duct using different nanofluids has been conducted by few researchers. The effects of Reynolds number ($75 \leq Re \leq 225$), temperature difference ($0 \leq \Delta T \leq 30$ °C), and nanofluid type (such as Au, Ag, Al_2O_3, Cu, CuO, diamond, SiO_2, and TiO_2) were investigated on the fluid flow and heat transfer characteristics. It is found that a recirculation region developed straight behind the backward-facing step which appeared between the edge of the step and few millimeters before the corner which connects the step and the downstream wall. In the few millimeters zone between the recirculation region and the downstream wall, a U-turn flow was developed opposite to the recirculation flow which is mixed with the unrecirculated flow and travels along the channel. Two maximum and one minimum peak in Nusselt number were observed along the heated downstream wall. It is inferred that Au nanofluid has the highest maximum peak of Nusselt number, while diamond nanofluid has the highest minimum peak in the recirculation region. Nanofluids with a higher Prandtl number have a higher maximum peak of Nusselt numbers after the separation and recirculation flow vanished.

The literature search indicates that the case of mixed laminar and turbulent convective flows over a horizontal forward-facing step having a baffle utilizing nanofluids has not been investigated yet and motivated the present study. Thus, the main objective of this study is to examine the heat transfer enhancement of 2D laminar and turbulent mixed convective flows adjacent to forward facing step with baffle installation onto the channel wall using different types of nanofluids.

2.0 NUMERICAL MODEL

2.1Physical Model

Two-dimensional laminar and turbulent mixed convection flows over forward facing step in a heated rectangular duct having a baffle mounted on the upper wall is numerically simulated, and the computational domain is schematically shown in Fig.1.

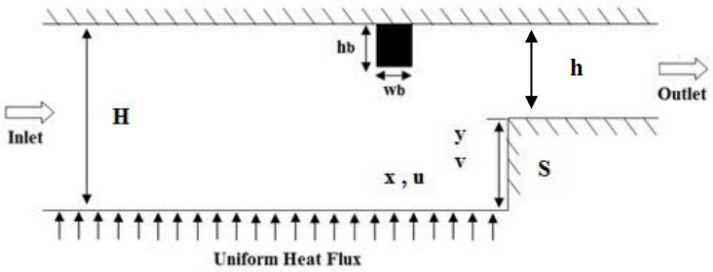

Figure 1: Schematic diagram of the computational domain of FFS with baffle installation

Journal of Advanced Research in Applied Mechanics
ISSN (online): 2289-7895 | Vol. 24, No. 1. Pages 1-21, 2016

The upstream height of the duct (h) is 0.01 m; its downstream height (H) is 0.02 m. This geometry provides a forward facing steps height (S) of 0.01 m, an expansion ratio of ER = H/ (H − S) = 2. A baffle is installed on the upper wall of the forward-facing step geometry and its relative position is shown in Figure1. Both the baffle's width (w_b) and height (h_b) are kept as 0.01 m. The length of the computational domain is 0.02 m and 0.5 m upstream and downstream of the sudden expansion respectively, i.e., $-2 \leq x/S \leq 50$.

Nanofluids flow at the channel entrance is considered to be hydrodynamically steady and the fully developed flow is attained at the edge of the step, and the streamwise gradients of all quantities at the channel exit where set to be zero.

The nanoparticles and the base fluid (water) are assumed to be in a thermal equilibrium and no slip condition occurs. The fluid flow is assumed to be Newtonian and incompressible. Radiation heat transfer and viscous dissipation term are neglected. The internal heat generation is not conducted in this study. The thermophysical properties of the nanofluids assumed to be constant and it is only affected by the buoyancy force, which means that the body force acting on the fluid is the gravity.

2.2 Governing Equations

The standard *k-ε* turbulent model was used for turbulence flow modeling. The conservation equations (continuity, momentum and energy equations) for steady flow, incompressible and Newtonian fluid can be written as follows [24]:

$$\frac{\partial u}{\partial x} + \frac{\partial v}{\partial y} = 0 \tag{1}$$

$$\rho\left(u\frac{\partial u}{\partial x} + v\frac{\partial u}{\partial y}\right) = -\frac{\partial p}{\partial x} + u\left(\frac{\partial^2 u}{\partial x^2} + \frac{\partial^2 u}{\partial y^2}\right) \tag{2}$$

$$\rho\left(u\frac{\partial v}{\partial x} + v\frac{\partial v}{\partial y}\right) = -\frac{\partial p}{\partial y} + u\left(\frac{\partial^2 v}{\partial x^2} + \frac{\partial^2 v}{\partial y^2}\right) \tag{3}$$

$$\rho\left(u\frac{\partial T}{\partial x} + v\frac{\partial T}{\partial y}\right) = \alpha\left(\frac{\partial^2 T}{\partial x^2} + \frac{\partial^2 T}{\partial y^2}\right) \tag{4}$$

$$\frac{\partial}{\partial x}(\rho k\mu) = \frac{\partial}{\partial y}\left(\left[\left(\mu + \frac{\mu_t}{\sigma_k}\right)\frac{\partial k}{\partial y}\right]\right) + G_k - \rho_\varepsilon \tag{5}$$

$$\frac{\partial}{\partial x}(\rho\varepsilon\mu) = \frac{\partial}{\partial y}\left[\left(\mu + \frac{\mu_t}{\sigma_\varepsilon}\right)\frac{\partial \varepsilon}{\partial y}\right] + C_{1\varepsilon}\frac{\varepsilon}{k}(G_k + C_{3\varepsilon}G_b) - C_{2\varepsilon}\rho\frac{\varepsilon^2}{k} \tag{6}$$

$C_{1\varepsilon}, C_{2\varepsilon}$, and $C_{3\varepsilon}$. σ_k and σ_ε are the turbulent pr numbers for k and ε respectively. The model constants are 1.44, 1.92, 0.09, 1.0 and 1.3 for $C_{1\varepsilon}$, $C_{2\varepsilon}$, C_μ, σ_k and σ_ε, respectively.

2.3 Boundary Conditions

The physical system under consideration, as shown in Figure.1 is a two-dimensional, horizontal channel with an abrupt compression in channel plate spacing at x= 0. The surfaces of the forward facing step are insulated; a portion of the bottom wall behind the step is subjected to a uniform heat flux. Besides, the rest portions of the bottom plate and the wall of the upper plate are well insulated. Flow enters the channel with a parabolic velocity profile and uniform temperature at the channel inlet far upstream of the step and fully-developed hydrodynamic and thermal conditions at the exit far downstream of the heating section of bottom plate. It is well known that the flow separation and recirculation cause very poor heat transfer characteristics in the region near the step. To alter the hydrodynamic and thermal characteristics, a baffle is introduced onto the upper plate of the channel. It is expected that the

Penerbit Akademia Baru
Journal of Advanced Research in Applied Mechanics
ISSN (online): 2289-7895 | Vol. 24, No. 1. Pages 1-21, 2016

baffle would strongly affect the velocity and temperature distributions of the flow. The no-slip conditions on all the solid walls, and the assumption of thermal insulation for the channel plates except the heating section of the bottom plate is considered [13].

2.3 Code Validation and Grid Testing

2.3.1 Grid Independence Test

Grid independence test is carried out to obtain the most suitable computational grid. Four different computational grids are considered, which are 180×40, 180×50, 200×50 and 250×60. All four grids are used to plot the velocity, temperature and the surface Nusselt number at downstream of the duct. As shown clearly in Figure 2, that all the four grids have similar results. However, any grid can be used. Thus, the grid of 180×50 is used as the best in terms of both the computational time and accuracy.

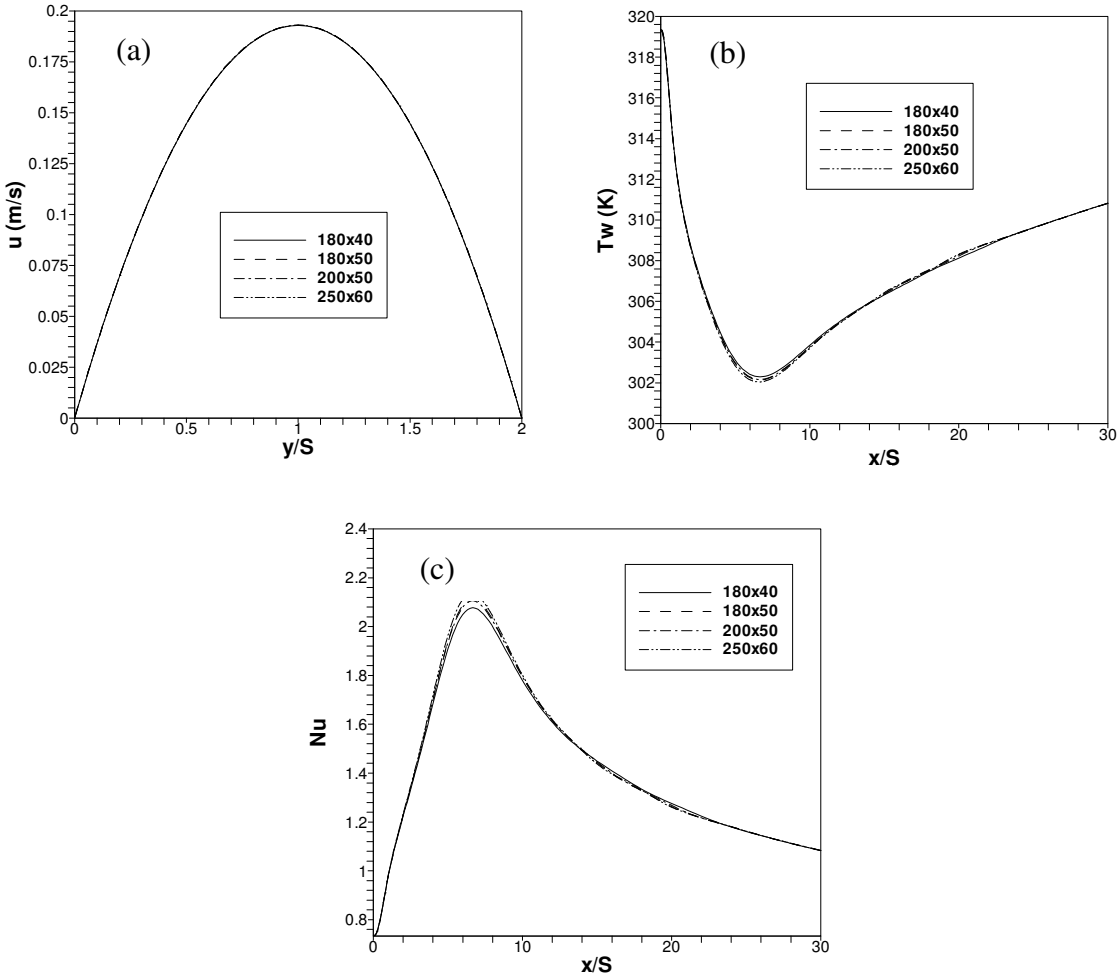

Figure 2: Grid independence test results for, (a) Velocity distribution, (b) Wall temperature distribution, (c) Nusselt number distribution, along the downstream

Penerbit Akademia Baru

Journal of Advanced Research in Applied Mechanics
ISSN (online): 2289-7895 | Vol. 24, No. 1. Pages 1-21, 2016

2.4.2 Code Validation

The numerical validation method involves the simulation of numerical codes under specific conditions for benchmark problems. The results of these simulations are compared with the theoretical and numerical data reported in the literature. It should give same results or very close to the previous works that have been investigated.

For validating the current results, the study done by Nie et al. [22] was used. Their research focused on numerical simulations of laminar mixed convection flow adjacent to back-ward facing step in rectangular duct to examine effects of the baffle on flow and heat transfer distributions as shown in Figure.3. In addition, another study of Tsay et al. [13] was selected to be surer of code validation. In this study, the heat transfer enhancement of back-ward facing step flow in a channel with the baffle installation on the channel wall was also used for comparison as shown in Figure.4 and Figure.5.

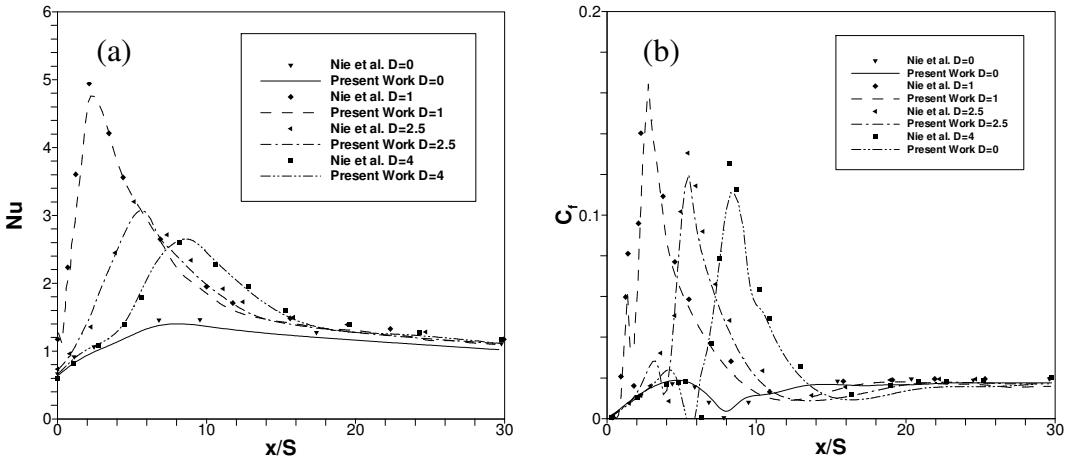

Figure 3: Comparison of the present work with the results of Nie et al. [22] for Re = 343 and $q_w = 50$ W/m^2 for, (a) Nusselt number, (b) Skin friction coefficient

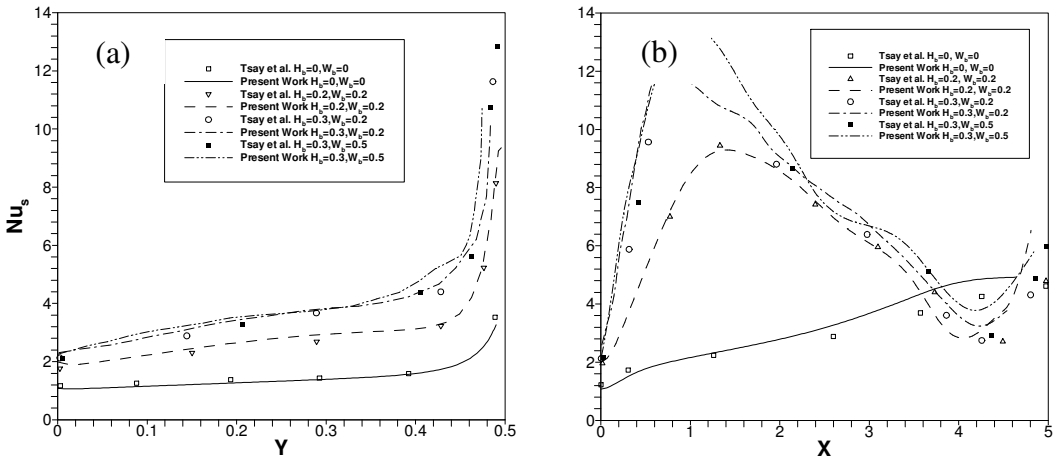

Figure 4: Comparison of the present work with the results of Tsay et al. [13] for Re=500, Gr/Re^2=1, D=0.2 for, (a) heating backward facing-step, (b) heating section of bottom plate

Penerbit Akademia Baru
Journal of Advanced Research in Applied Mechanics
ISSN (online): 2289-7895 | Vol. 24, No. 1. Pages 1-21, 2016

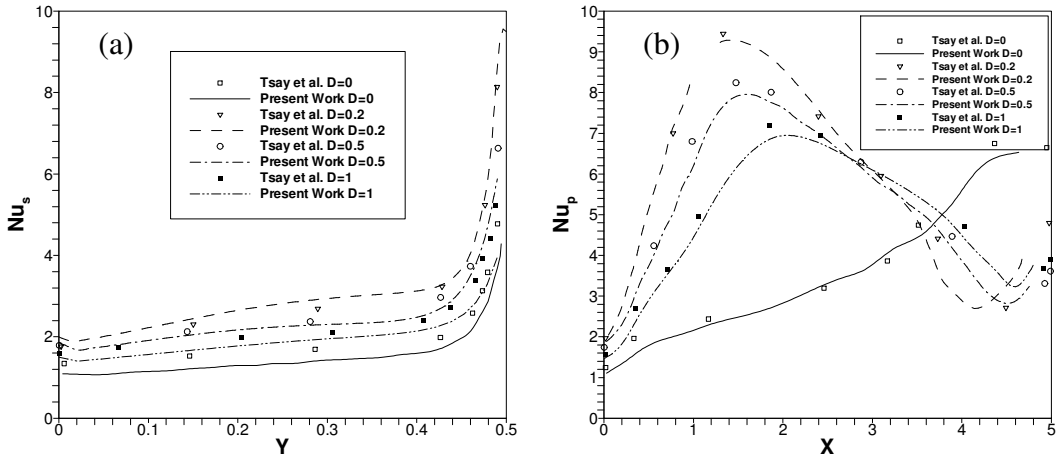

Figure 5: Comparison of the present work with the results of Tsay et al. [13] for Re=500, Gr/Re^2=1, H_b=0.2, W_b=0.2, for, (a) heating backward facing-step, (b) heating section of bottom plate

Distributions of the Nusselt number at the heated stepped wall are presented in Figure 3a. The maximum Nusselt number develops near to side-wall, and it moves further downstream as the location of the baffle moves along the streamwise direction. The distribution of the friction coefficient at the stepped wall along the duct is shown in Figure 3b. Figure 4 depicts the heat transfer characteristics for the heating step and the heating section of the bottom wall, respectively. Figure 5 represents the Nusselt number for the system with $H_b = 0.2$ and $W_b = 0.2$ at four different values of D.

2.5 Numerical Parameters and Procedures

The numerical computation was carried out by solving the governing conservation equations along with the boundary conditions Equations (1) to (6). Equations for solid and fluid phase were simultaneously solved as a single domain. The discretization of governing equations in the fluid and solid regions was done using the finite-volume method (FVM). The diffusion term in the momentum and energy equations is approximated by second-order central difference which gives a stable solution. In addition, a second-order upwind differencing scheme is adopted for the convective terms. The numerical model was developed in the physical domain, and dimensionless parameters were calculated from the computed velocity and temperature distributions. The flow field was solved using the SIMPLE algorithm [25]. This is an iterative solution procedure where the computation is initialized by guessing the pressure field. Then, the momentum equation is solved to determine the velocity components. The pressure is updated using the continuity equation. Even though the continuity equation does not contain any pressure, it can be transformed easily into a pressure correction equation [26].

Quadrilateral elements and a non-uniform grid system are employed in the simulations. The grid is highly concentrated close to the step, and near the step edge and walls, to ensure the accuracy of the numerical simulations and for saving both the grid size and computational time. At the each iteration end, the residual sum for each of the conserved variables is computed and stored, thus recording the convergence history. The convergence criterion required that the maximum relative mass residual based on the inlet mass be smaller than 1×10^{-3}.

Journal of Advanced Research in Applied Mechanics
ISSN (online): 2289-7895 | Vol. 24, No. 1. Pages 1-21, 2016

2.6 Thermophysical Properties of Nanofluids

The effective thermophysical properties of nanofluids must be calculated first to carry out simulations for nanofluids. The nanoparticles being used are $A1_2O_3$, CuO, SiO_2, and ZnO. Basically the required properties for the simulations are effective thermal conductivity (k_{eff}), effective dynamic viscosity (μ_{eff}), effective mass density (ρ_{eff}), effective coefficient of thermal expansion(β_{eff}) and effective specific heat ($Cp_{,eff}$). The effective properties of mass density, specific heat and coefficient of thermal expansion are actually calculated according to the mixing theory.

By using Brownian motion of nanoparticles in forward facing step having a baffle, the effect thermal conductivity can be obtained as following mean empirical correlation [27]:

$$k_{eff} = k_{Static} + k_{Brownian} \quad (7)$$

Static Thermal Conductivity:

$$k_{Static} = k_{bf}\left[\frac{k_{np}+2k_{bf}-2(k_{bf}-k_{np})\emptyset}{k_{np}+2k_{bf}+(k_{bf}-k_{np})\emptyset}\right] \quad (7.1)$$

Brownian Thermal Conductivity:

$$k_{Brownian} = 5x10^4\beta\emptyset\rho_{bf}c_{p,bf}\sqrt{\frac{\kappa T}{2\rho_{np}R_{np}}}.f(T,\emptyset) \quad (7.2)$$

When:
Boltzmann constant:

$$k = 1.3807x10^{-23}\ J/K$$

Modeling function, β [28]:

$$\beta = 0.0137(100\emptyset)^{-0.8229} \text{ for } \emptyset < 1\%$$
$$\beta = 0.0011(100\emptyset)^{-0.7272} \text{ for } \emptyset > 1\%$$

Modeling function, f (T, Ø): $f(T,\emptyset) = (2.8217x10^{-2}\emptyset) + 3.917x10^{-3})\left(\frac{T}{T_0}\right) + (-3.0699x10^{-2}\emptyset - 3.91123x10^{-3})$

By using Brownian motion of nanoparticles the effective viscosity can be obtained by using the following empirical correlation [29]:

Viscosity:

$$\frac{\mu_{eff}}{\mu_f} = \frac{1}{1-34.87\left(\frac{d_p}{d_f}\right)^{-0.3}\emptyset^{1.03}} \quad (8)$$

Equivalent diameter of base fluid molecule:

$$d_f = \left[\frac{6M}{N\pi\rho_{bf}}\right]^{1/3} \quad (9)$$

where Ø is the particle volume fraction, M is the molecular weight of the base fluid, N is the Avogadro number, *f* refers to nanofluid, *bf* refers to base fluid and *p* refers to Nanoparticle.

Journal of Advanced Research in Applied Mechanics
ISSN (online): 2289-7895 | Vol. 24, No. 1. Pages 1-21, 2016

- The density of the nanofluid ρ_{nf} can be calculated using [27]:

$$\rho_{nf} = (1 - \emptyset)\rho_f + \emptyset\rho_{np} \quad (10)$$

whereby ρ_f and ρ_{np} are the mass densities of the base fluid and the solid nanoparticles, respectively.

- The effect Heat capacity at constant pressure of the nanofluid $(\rho c_p)_{nf}$ can be calculated using [27]:

$$(\rho c_p)_{nf} = (1 - \emptyset)(\rho c_p)_f + \emptyset(\rho c_p)_{np} \quad (11)$$

where $(c_p)_f$ and $(c_p)_{np}$ are heat capacities of base fluid and nanoparticles, respectively.

- The effect coefficient of thermal expansion of nanofluid $(\rho\beta)_{nf}$ can be calculated using [27]:

$$(\rho\beta)_{nf} = (1 - \emptyset)(\rho\beta)_f + \emptyset(\rho\beta)_{np} \quad (12)$$

when $(\beta)_f$ and $(\beta)_{np}$ are thermal expansion coefficients of base fluid and nanoparticles, respectively.

3.0 RESULTS AND DISCUSSION

The effects of different nanofluid type, its concentration and particles diameter, Reynolds number and baffle geometrical parameters on the thermal and flow fields over backward facing step are analyzed and discussed in this section.

3.1 The Effect of Different Types of Nanoparticles

The velocity distributions of different nanofluids over forward-facing step with φ = 4% for *Re* = 300, *D* = 1 and *q* = 50 W/m^2 for different *x/S* sections along the downstream wall are shown in Figure 6a-b. It is clear from the figures at *x/S* = 1 and *x/S* = 30 that nanofluids with low density such as SiO_2 have higher velocity distribution at the edge of the baffle wall than those with high density such as CuO at constant Reynolds number. The opposite flow is observed behind the step wall due to the recirculation region that attached to the step and the second is the vortex which leaves the recirculation region and changes its direction downstream the channel duo to the buoyancy force.

The distributions of Nusselt number of different nanofluids with volume fraction (φ = 4%) at *D* = 1, *Re* = 300 and *q* = 50 w/m^2 are shown in Figure 6c. The figure shows that all nanofluids possess higher Nusselt number compared to water, and nanofluids are richer in heat transfer rate than the pure water. But in case of comparing among the nanofluids, the nanofluid with SiO_2 has the best heat transfer enhancement, followed by Al_2O_3, ZnO and CuO respectively. Nanofluids with high density and low specific heat capacity have higher Nusselt number while nanofluids with low density and high specific heat capacity have lower Nusselt number. However, this case is not applicable for SiO_2 due to the large differences in its thermophysical properties compared to other nanofluids.

Penerbit Akademia Baru
Journal of Advanced Research in Applied Mechanics
ISSN (online): 2289-7895 | Vol. 24, No. 1. Pages 1-21, 2016

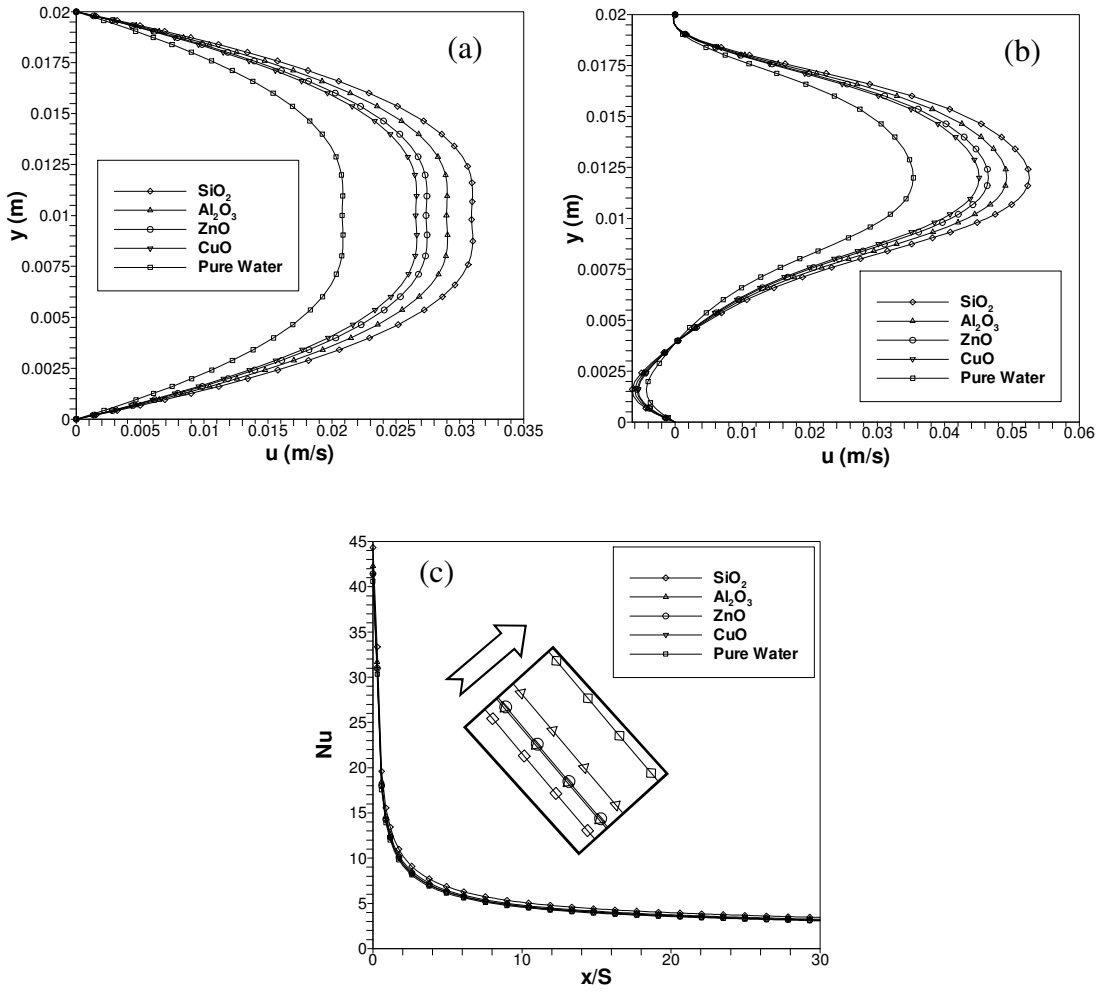

Figure 6: Effect of different nanofluids with $\varphi = 4\%$ for $Re = 300$, $D = 1$ and $q = 50\text{W/m}^2$, (a) Velocity distribution of $x/S = 1$, (b) Velocity distribution of $x/S = 30$, (c) Nusselt number distributions

3.2 Effect of Different Nanoparticles Volume Fractions

The velocity distributions over forward-facing step of different nanoparticles volume fractions for $Re = 300$, $D = 1$ and $q = 50\ \text{W/m}^2$ for different x/S sections along the downstream wall are shown in Figure 7a-b. The results investigate that with increasing of volume fraction leads to enhance the effective properties of the nanoparticles. In this case, the velocity distribution increases as volume fraction of nanoparticles increases.

The relations for volume concentration of nanoparticles in base fluid and/or nanofluids have been developed based on conservation of mass and assumed conservation of mixture volume of its components. In this study the volume fraction in the range of 0 - 4% with fixed $D = 1$, $Re = 300$ and $q = 50\ \text{W/m}^2$. The results indicate that with increasing of volume fraction leads to enhance the effective properties of the nanoparticles as shown in Figure 7c. Nanofluids with higher volume fraction give greater heat transfer enhancement, because increasing volume fraction of nanofluids lead to increase the thermal conductivity of the fluid.

Penerbit Akademia Baru
Journal of Advanced Research in Applied Mechanics
ISSN (online): 2289-7895 | Vol. 24, No. 1. Pages 1-21, 2016

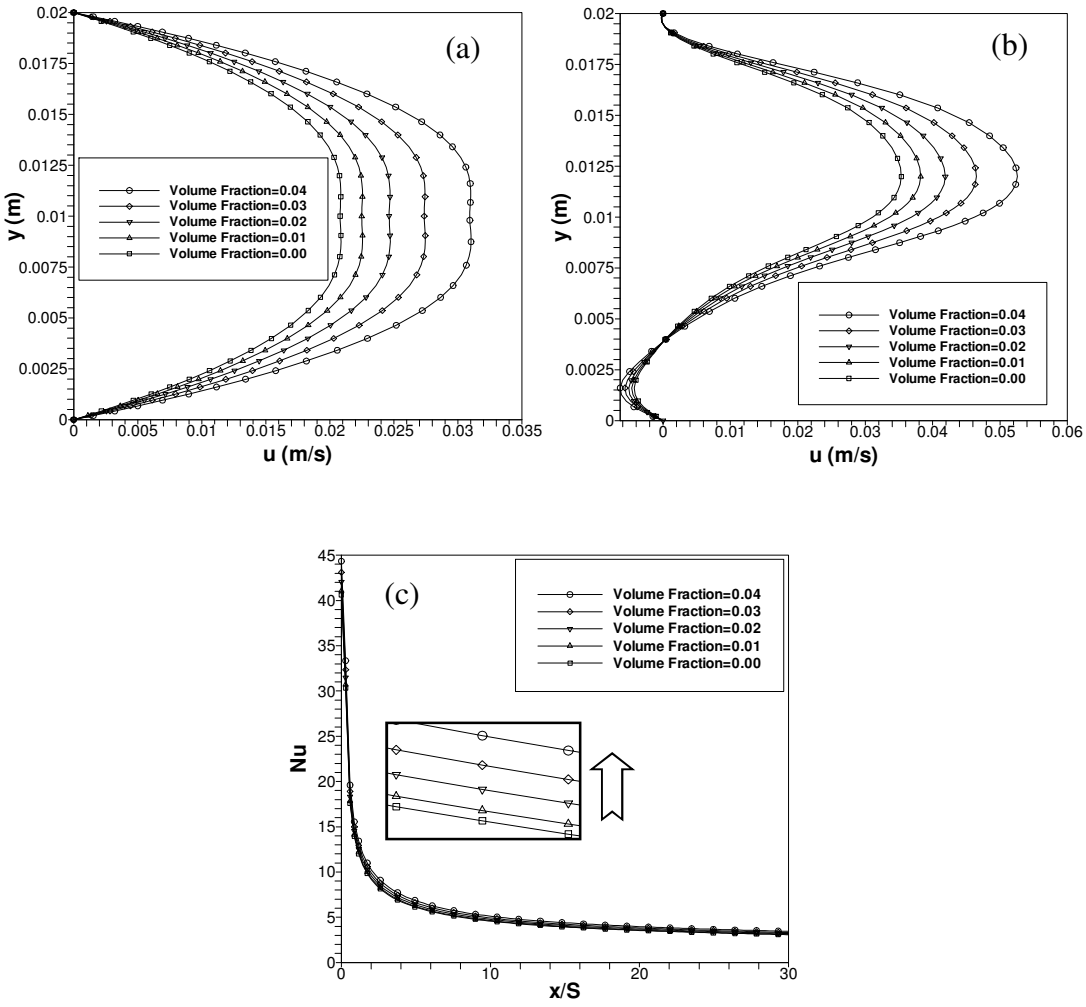

Figure 7: Effect of different nanoparticles volume fractions for Re = 300, D = 1 and q = 50W/m^2 (a) Velocity distribution of x/S = 1, (b) Velocity distribution of x/S = 30, (c) Nusselt number distributions

3.3 The Effect of Different Nanoparticles Diameters

The velocity profiles of Re = 300, D = 1 and q = 50W/m^2 with φ = 4% for different nanoparticles diameters at different positions of downstream wall over forward-facing step is shown in Figure 8a-b. It is found that the base-fluid with low nanoparticles diameter such as d_p = 25 nm has a higher parabolic flow in the streamwise direction on the edge of the step. It is included that all the selected nanoparticles diameters have a primary recirculation region.

This study is used SiO_2-water (φ = 4%) as a working-fluid with fixed other parameters such as Re = 300, q = 50 W/m^2 and D = 1. The range of nanoparticles diameter is 25-80 nm. As illustrated in Figure 8c, the results of forward-facing step show that the Nusselt number increases with decreasing the nanoparticles diameter. This can be attributed to the increment of the thermal conductivity due to nanoparticles diameter decreases. The properties of nanofluid come from high surface area to the volume ratio. As heat transfer focused on the surface of the nanoparticles, it desirable to use particles that possess high surface area to volume ratio. Thus, it is concluded that by using smaller diameter of nanoparticles will get better heat transfer enhancement.

Penerbit Akademia Baru
Journal of Advanced Research in Applied Mechanics
ISSN (online): 2289-7895 | Vol. 24, No. 1. Pages 1-21, 2016

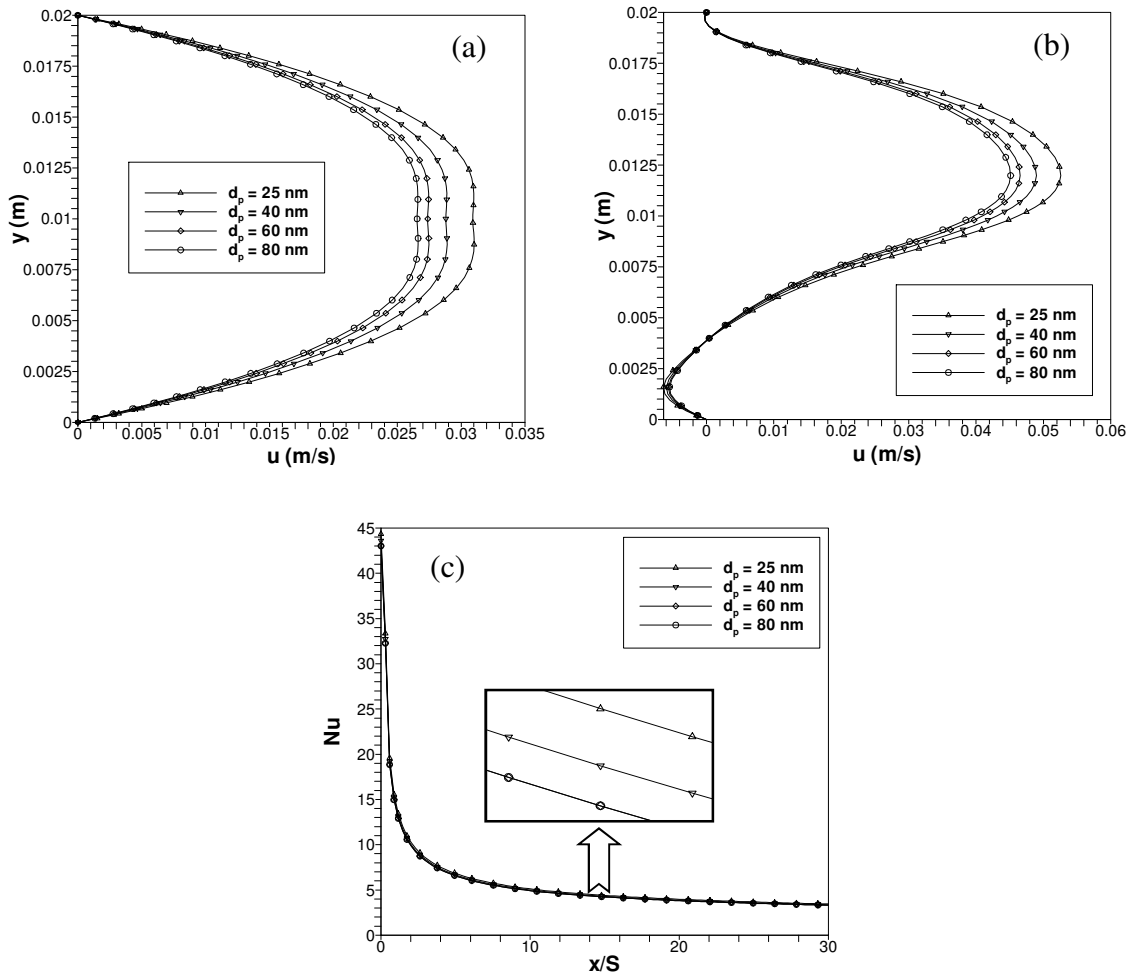

Figure 8: Effect of different nanoparticles diameters with $\varphi = 4\%$ for $Re = 300$, $D = 1$ and $q = 50 W/m^2$ (a) Velocity distribution of $x/S = 1$, (b) Velocity distribution of $x/S = 30$, (c) Nusselt number distributions

3.4 Effect of Different Reynolds Numbers

3.4.1 Laminar Flow

The velocity distributions for different Reynolds numbers (laminar flow) over forward facing step with $\varphi = 4\%$, $D = 1$ and $q = 50$ W/m^2 at different x/S are shown in Figure 9a-b. The velocity profile increases as Reynolds number increases. The recirculation is found to increase as Reynolds number increases and vice versa.

The skin friction coefficient for different Reynolds numbers (laminar flow) over forward facing step with $\varphi = 4\%$, D=1 and q=50 W/m^2 along the downstream wall is shown in Figure 9c. It is observed that the skin friction coefficient decreases as Reynolds number increases. This is because the velocity is directly proportional to Reynolds number, and inversely proportional to skin friction coefficient.

This study was done at Reynolds number in the range of 100 - 500 with $\varphi = 4\%$, $D = 1$ and $q = 50$ W/m^2 for the flow over forward-facing step. As shown in Figure 9d, the Nusselt number

Penerbit Akademia Baru
Journal of Advanced Research in Applied Mechanics
ISSN (online): 2289-7895 | Vol. 24, No. 1. Pages 1-21, 2016

increases as Reynolds number increases. The maximum Nusselt number occurs at the inlet of the duct, and then it reaches the minimum value at the step wall due to the temperature difference.

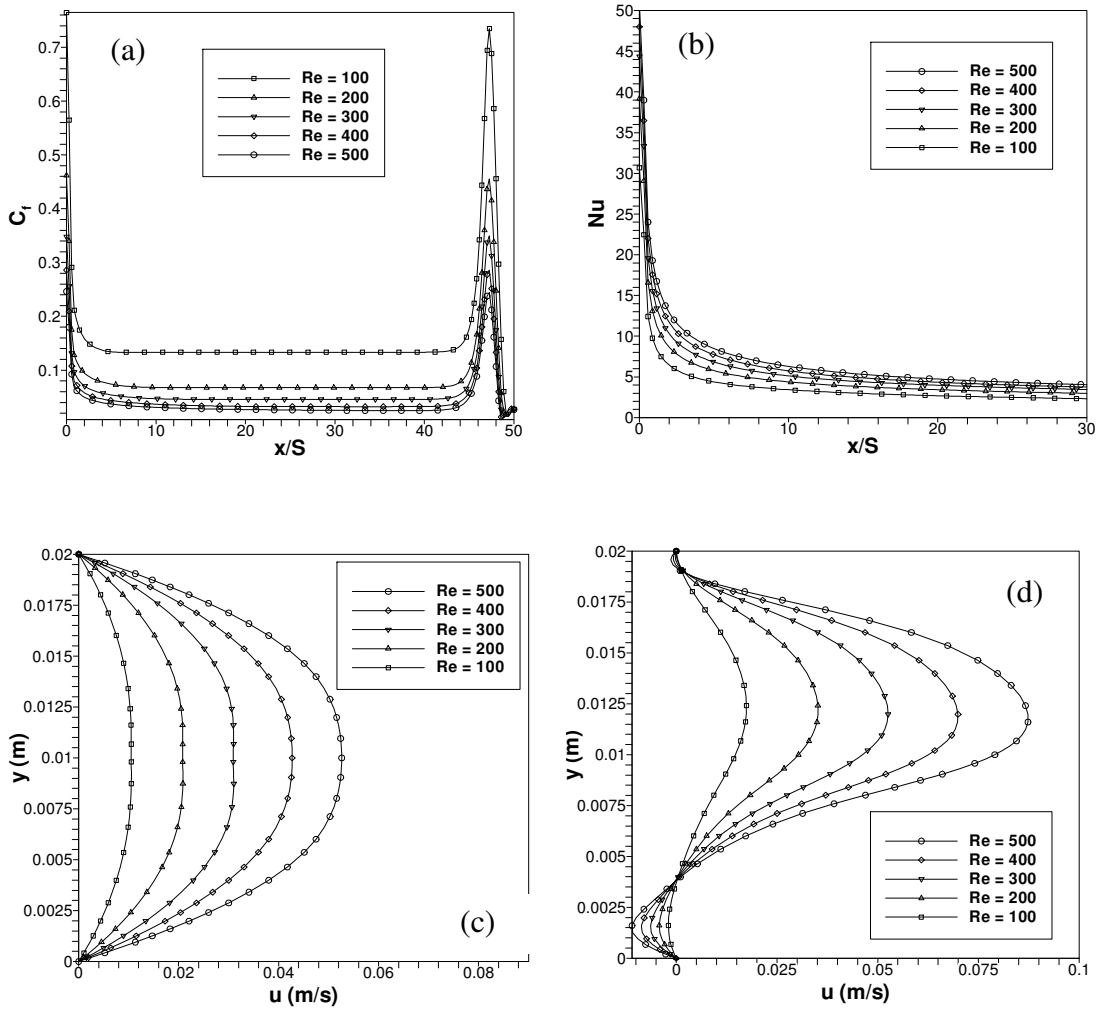

Figure 9: Laminar flow with $\varphi = 4\%$ for $D = 1$ and $q = 50 W/m^2$ (a) Velocity distribution of $x/S = 1$, (b) Velocity distribution of $x/S = 30$, (c) Skin friction coefficient, (d) Nusselt number distributions

3.4.2 Turbulent Flow

The velocity distributions of different Reynolds numbers (turbulent flow) with $\varphi = 4\%$, $D = 1$ and $q = 50$ W/m^2 at different x/S are shown in Figure 10a-b. The velocity profile increases as Reynolds number increases. In this section two section are examined which are $x/S = 1$ (before the baffle) and $x/S = 30$ (between the baffle and the step wall).

The skin friction coefficient of turbulent flow for different Reynolds numbers with $\varphi = 4\%$, $D = 1$ and $q = 50$ W/m^2 along the downstream wall is shown in Figure 10c. It is observed that the skin friction coefficient decreases as Reynolds number increases. This is because the velocity is directly proportional to Reynolds number, and inversely proportional to skin friction coefficient.

Penerbit Akademia Baru
Journal of Advanced Research in Applied Mechanics
ISSN (online): 2289-7895 | Vol. 24, No. 1. Pages 1-21, 2016

The Nusselt number of turbulent flow over forward facing step at different Reynolds numbers with $\varphi = 4\%$, $D = 1$ and q=50 W/m^2 is shown in Figure 10d. It is found that the first maximum peak of Nusselt number is occurred in the inlet of the duct, and the second maximum peak at the step wall. In addition, it is noticed that the Nusselt number increases as Reynolds number increases.

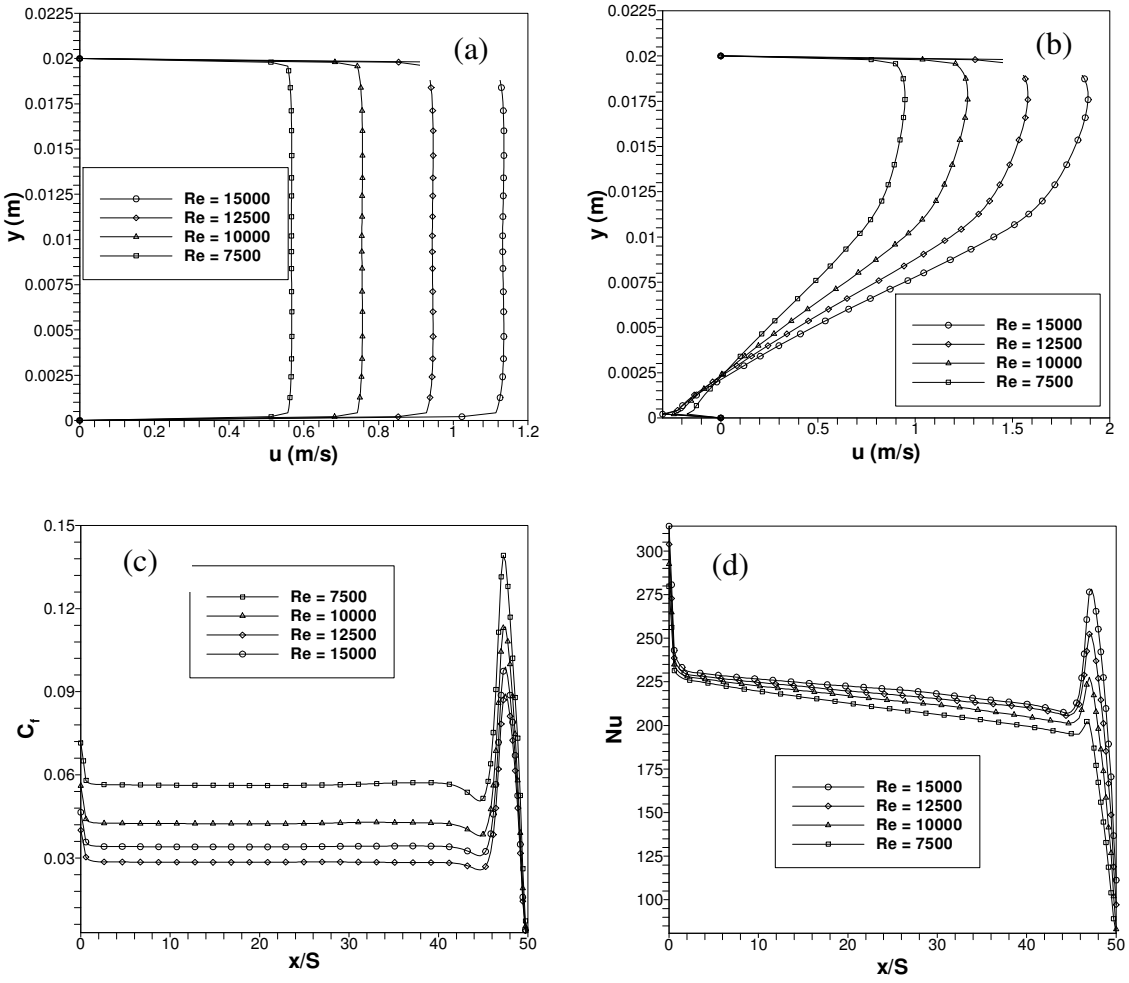

Figure 10: Turbulent flow with $\varphi = 4\%$ for $D = 1$ and $q = 50\text{W/m}^2$ (a) Velocity distribution of $x/S = 1$, (b) Velocity distribution of $x/S = 30$, (c) Skin friction coefficient, (d) Nusselt number distributions

3.5 The Effect of Geometrical Parameters

3.5.1 Effect of Baffle Distance

The Nusselt number for different baffle distances of the flow over forward facing step along the top-wall with $\varphi = 4\%$, $Re = 300$ and $q = 50$ W/m^2 is shown in Figure 11. Because of the applied boundary condition of constant heat flux, the maximum Nusselt number is inversely proportional to the minimum wall temperature. The magnitude of the maximum Nusselt number increases as the baffle moves towards the forward-facing step (with the decrease of D).

Penerbit Akademia Baru

Journal of Advanced Research in Applied Mechanics
ISSN (online): 2289-7895 | Vol. 24, No. 1. Pages 1-21, 2016

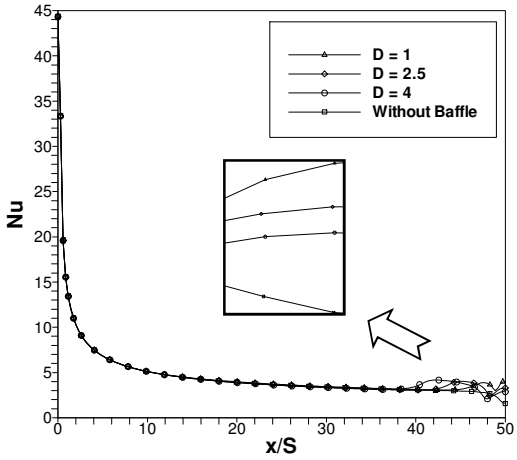

Figure 11: Nusselt number for different baffle distances with $\varphi = 4\%$, $Re = 300$ and $q = 50\text{W/m}^2$

3.5.2 Effect of Baffle Width

The velocity distributions for different baffle widths for the flow over forward facing step with $D = 1$, $Re = 300$ and $q = 50$ W/m^2 is shown in Figure 12a. All four cases of baffle width are slightly different to each other's, as shown in skin friction coefficient effect the case of $W_b = 0.01$ gives the best velocity profile.

The skin friction coefficient at $D = 1$, $Re = 300$ and $q = 50$ W/m^2 for different baffle width is illustrated in Figure 12b. From the second maximum value of skin friction, the case of $W_b = 0.01$ shows the best value followed by the case $W_b = 0.02$, Wb = 0.03 and $W_b = 0.04$. Thus, the lowest width of baffle gives the better heat transfer enhancement for the flow over forward-facing step due to the skin friction coefficient is inversely proportional to the velocity.

Nusselt number of the flow over forward-facing step for different baffle width at $D = 1$, $Re = 300$ and $q = 50$ W/m^2 is shown in Figure 12c. It is found that the effect of baffle width on the Nusselt number is insignificant. For all four cases, the Nusselt number is starting with peak value at the duct inlet, and it decreases along the downstream wall.

3.5.3 Effect of Baffle Height

Skin friction coefficient for different baffle heights for the flow over forward facing step was significant to investigate the effect of baffle height on the heat transfer enhancement. As shown in Figure 13a, the skin friction coefficient increases as the baffle height increases. It is concluded that the less baffle height gives high heat transfer characteristics.

The Nusselt number of different baffle heights with $D = 1$, $Re = 300$ and $q = 50\text{W/m}^2$ for the flow over forward facing step is shown in Figure 13b. It is found that the effect of baffle height on the Nusselt number is insignificant. For all three cases, the Nusselt number is starting with peak value at the duct inlet, and it decreases along the downstream wall.

Penerbit Akademia Baru

Journal of Advanced Research in Applied Mechanics
ISSN (online): 2289-7895 | Vol. 24, No. 1. Pages 1-21, 2016

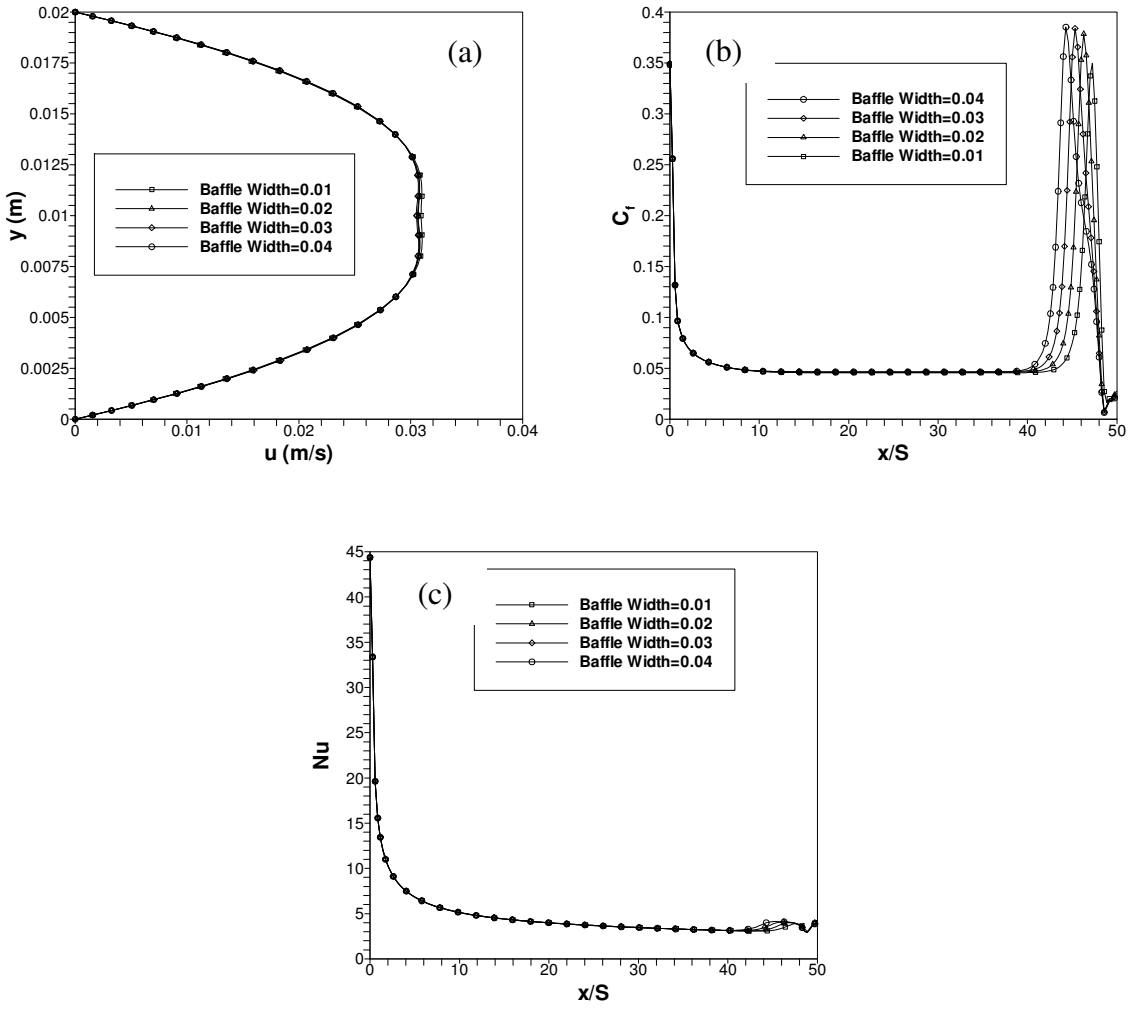

Figure 12: Effect of baffle widths on the stepped wall along the center of the duct with φ = 4% for Re = 300 and q = 50W/m^2 (a) Velocity distributions at x/S=1 (b) Skin friction coefficient, (c) Nusselt number distributions

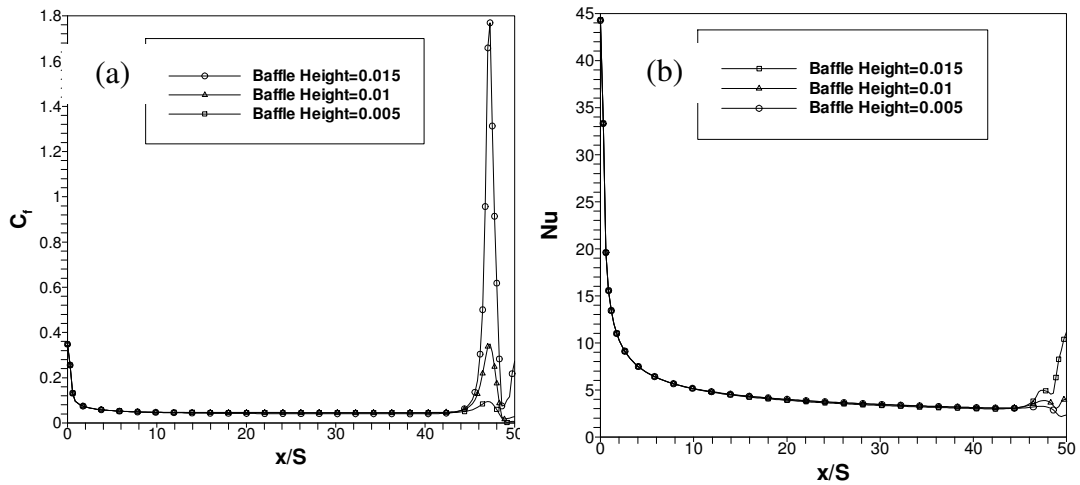

Figure 13: The effect of baffle heights on the stepped wall along the center of the duct with D = 1, Re = 300 and q = 50W/m^2, (a) Skin friction coefficient distributions, (b) Nusselt number distributions

Penerbit Akademia Baru

Journal of Advanced Research in Applied Mechanics
ISSN (online): 2289-7895 | Vol. 24, No. 1. Pages 1-21, 2016

3.5.4 Effect of Baffle Number

The velocity distribution for different baffle numbers with Re = 300 and q = 50 W/m^2 along the top-wall of duct is shown in Figure 14a. It is clearly that the baffle number has a slight effect in velocity profile. As shown in velocity distribution at x/S = 30, the velocity profile increases as the baffle number increases.

Skin friction coefficient for different baffle numbers for the flow over forward facing step was significant to investigate the effect of baffle number on the heat transfer enhancement. As shown in Figure 14b, the skin friction coefficient increases as the baffle number increases due to the velocity decreasing.

The Nusselt number of different baffle numbers with D = 1, Re = 300 and q = 50W/m^2 for the flow over forward facing step is shown in Figure 14c. It is found that the effect of baffle number on the Nusselt number is insignificant. For all three cases, the Nusselt number is starting with peak value at the duct inlet, and it decreases along the downstream wall.

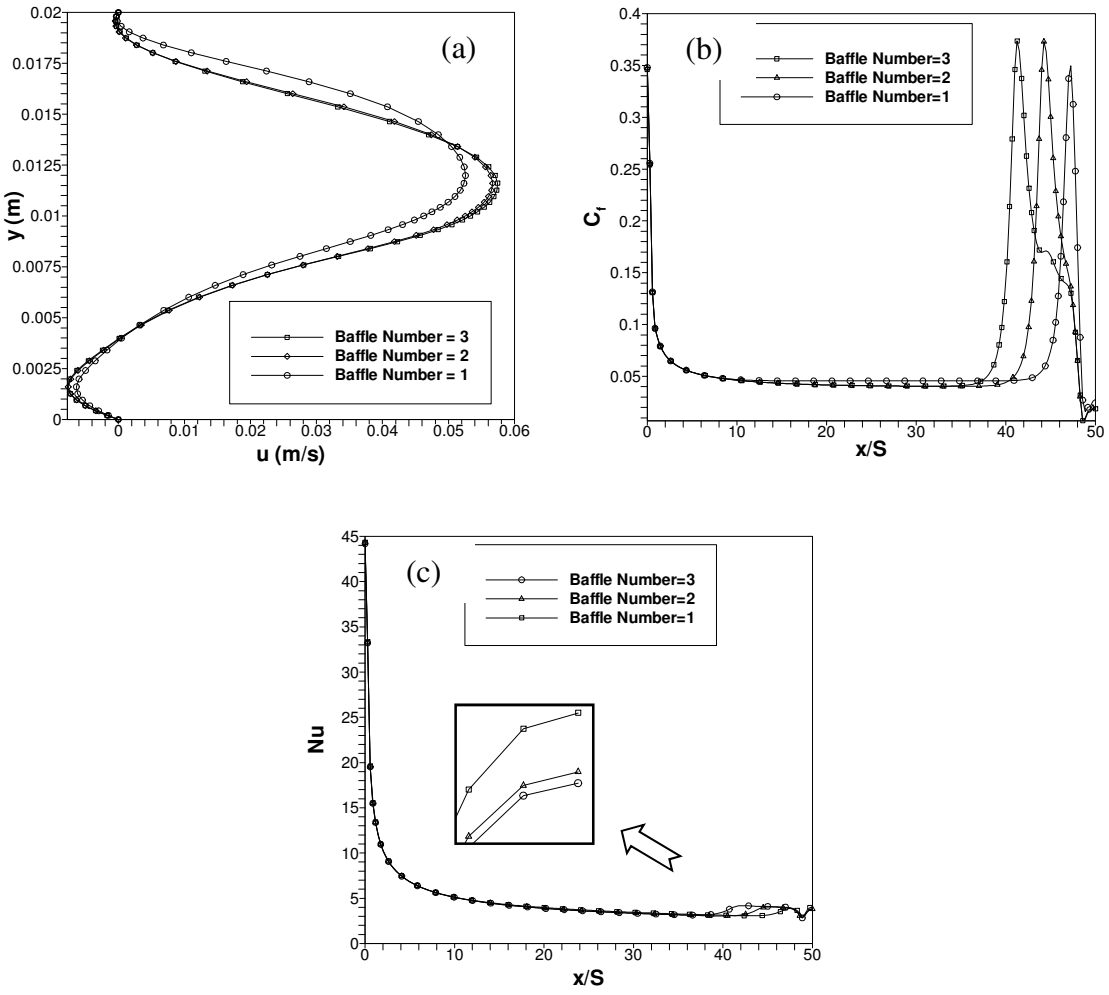

Figure 14: Effect of baffle numbers on the stepped wall along the center of the duct with D = 1, Re = 300 and q = 50W/m^2, (a) Velocity distributions at x/S=30, (b) The Skin friction coefficient distributions, (c) Nusselt number distributions

Penerbit Akademia Baru

Journal of Advanced Research in Applied Mechanics
ISSN (online): 2289-7895 | Vol. 24, No. 1. Pages 1-21, 2016

3.5.5 Effect of Baffle Location

The velocity distributions of forward-facing step for two locations of baffle with fixed other parameters such as $D = 1$, $Re = 300$ and $q = 50$ W/m^2 are shown in Figure 15a-b. The results show that baffle installation at the down-wall is slightly better than baffle installation at the top-wall. In addition the velocity profile of baffle installation at down-wall develops at the section $x/S = 1$. The velocity profile of $x/S = 30$ gives significant effect of baffle location.

The skin friction of forward-facing step for two locations of baffle with fixed other parameters such as $D = 1$, $Re = 300$ and $q = 50$ W/m^2 is shown in Figure 15c. The results show that baffle installation at the down-wall is clearly better than baffle installation at the top-wall due to the velocity of these two locations.

The Nusselt number of different baffle locations with $D = 1$, $Re = 300$ and $q = 50$W/m^2 for the flow over forward facing step is shown in Figure 15d. It is found that the effect of baffle location on the Nusselt number is insignificant. For the two cases, the Nusselt number is starting with peak value at the duct inlet, and it decreases along the downstream wall.

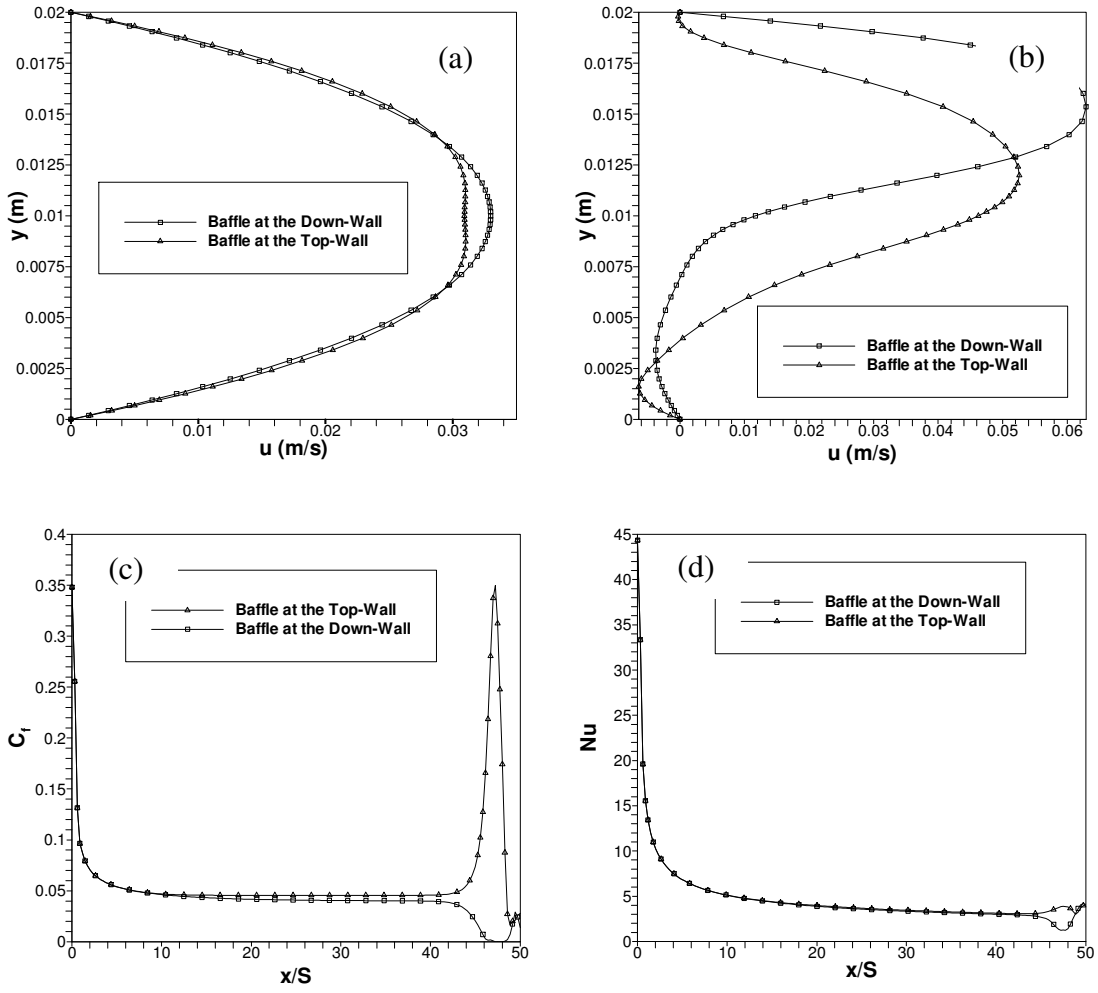

Figure 15: Effect of baffle locations on the stepped wall along the center of the duct with D = 1, Re = 300 and q = 50W/m^2, (a) Velocity distributions at x/S=1, (b) Velocity distributions at *x/S*=30, (c) The Skin friction coefficient distributions, (d) Nusselt number distributions

4.0 CONCLUSION

Numerical simulation of laminar and turbulent mixed convection heat transfer of nanofluids flow over forward facing step placed in a horizontal duct having baffle at its wall was carried out. The emphasis is given on the heat transfer enhancement resulting from various parameters, which include the different type of nanofluids, volume fraction of nanoparticles, nanoparticles diameter, baffle geometrical parameters and the Reynolds number. The governing equations were solved utilizing finite volume method with the SIMPLE algorithm. The following conclusions can be drawn from this study as follows:

- The results show that SiO_2 gives the highest Nusselt number and velocity distribution followed by Al_2O_3, ZnO and CuO respectively, while pure water is the lowest.
- The Nusselt number and velocity distribution increased with increasing the volume friction on nanoparticles.
- The Nusselt number and velocity profile decreased with increasing the diameter of nanoparticles.
- The Nusselt number and velocity distribution increased gradually by increasing the Reynolds number of laminar and turbulent flows, and vice versa for the skin friction.
- A slight movement of the baffle could cause a drastic change in the flow structure and temperature distributions. The optimum position of the baffle installation for heat transfer enhancement varies with the specified thermal and flow conditions.
- The effects of baffle widths and baffle numbers on heat transfer are insignificant.
- The heat transfer characteristics improved as the height of baffle increased.
- Installation of a baffle at the upper wall enhances heat transfer and increases the magnitude of maximum Nusselt number at the stepped wall. Baffle at bottom-wall in backward-facing step showed good enhancement of heat transfer.

REFERENCES

[1] Alawi, O. A., Che Sidik, N. A., Kazi, S. N., Abdolbaqi, M. Kh. " Comparative Study on Heat Transfer Enhancement and Nanofluids Flow over Backward and Forward Facing Steps." Journal of Advanced Research in Fluid Mechanics and Thermal Sciences 23, no. 1 (2016): 25-46.

[2] Daungthongsuk, Weerapun, and Somchai Wongwises. "A critical review of convective heat transfer of nanofluids." Renewable and Sustainable Energy Reviews 11, no. 5 (2007): 797-817.

[3] Khattak, M. A., A. Mukhtar, and S. Kamran Afaq. "Application of Nano-Fluids as Coolant in Heat Exchangers: A Review." J. Adv. Rev. Sci. Res 22, no. 1 (2016): 1-11.

[4] Nor Azwadi, C. S., Adamu, I. M. and Jamil, M. M. " Preparation Methods and Thermal Performance of Hybrid Nanofluids." J. Adv. Rev. Sci. Res 24, no. 1 (2016): 13-23.

[5] Sinz, C. K., Woei, H. E., Khalis M. N. and Ali Abbas, S. I. " Numerical Study on Turbulent Force Convective Heat Transfer of Hybrid Nanofluid, Ag/HEG in a Circular Channel with Constant Heat Flux." Journal of Advanced Research in Fluid Mechanics and Thermal Sciences 24, no. 1 (2016): 1-11.

[6] Mohammed, H. A., A. A. Al-Aswadi, N. H. Shuaib, and R. Saidur. "Convective heat transfer and fluid flow study over a step using nanofluids: a review."Renewable and Sustainable Energy Reviews 15, no. 6 (2011): 2921-2939.

[7] Abu-Mulaweh, H. I., Bassem F. Armaly, and T. S. Chen. "Laminar natural convection flow over a vertical forward-facing step." Journal of thermophysics and heat transfer 10, no. 3 (1996): 517-523.

[8] Abdalla, Ibrahim Elrayah, Zhiyin Yang, and Malcolm Cook. "Computational analysis and flow structure of a transitional separated-reattached flow over a surface mounted obstacle and a forward-facing step." International Journal of Computational Fluid Dynamics 23, no. 1 (2009): 25-57.

[9] Stüer, Heinrich. "Investigation of separation on a forward facing step." PhD diss., Diss. Techn. Wiss. ETH Zürich, Nr. 13132, 1999. Ref.: W. Kinzelbach; Korref.: L. Kleiser; Korref.: A. Gyr, 1999.

[10] Abe, K., T. Kondoh, and Y. Nagano. "A new turbulence model for predicting fluid flow and heat transfer in separating and reattaching flows—I. Flow field calculations." International journal of heat and mass transfer 37, no. 1 (1994): 139-151.

[11] Ando, Toshitake, and Toshihiko Shakouchi. "Flow characteristics over forward facing step and through abrupt contraction pipe and drag reduction." Res. Rep. Fac. Eng. Mie Univ 29 (2004): 1-8.

[12] Ito, Kazufumi, and S. S. Ravindran. "A reduced-order method for simulation and control of fluid flows." Journal of computational physics 143, no. 2 (1998): 403-425.

[13] Tsay, Y-L., Tsai-Shou Chang, and Jen-Chieh Cheng. "Heat transfer enhancement of backward-facing step flow in a channel by using baffle installation on the channel wall." Acta mechanica 174, no. 1-2 (2005): 63-76.

[14] Berner, C., F. Durst, and D. M. McEligot. "Flow around baffles." Journal of heat transfer 106, no. 4 (1984): 743-749.

[15] Berner, C., F. Durst, and D. M. McEligot. "Streamwise-periodic flow around baffles." In Proceedings of the 2nd international conference on applications of laser anemometry to fluid mechanics, Lisbon, Portugal. 1984.

[16] Habib, M. A., A. M. Mobarak, M. A. Sallak, EA Abdel Hadi, and R. I. Affify. "Experimental investigation of heat transfer and flow over baffles of different heights." Journal of heat transfer 116, no. 2 (1994): 363-368.

[17] Webb, B. W., and S. Ramadhyani. "Conjugate heat transfer in a channel with staggered ribs." International Journal of Heat and Mass Transfer 28, no. 9 (1985): 1679-1687.

[18] Kelkar, K. M., and S. V. Patankar. "Numerical prediction of flow and heat transfer in a parallel plate channel with staggered fins." Journal of heat transfer 109, no. 1 (1987): 25-30.

[19] Habib, M. A., A. E. Attya, and D. M. McEligot. "Calculation of turbulent flow and heat transfer in channels with streamwise-periodic flow." Journal of turbomachinery 110, no. 3 (1988): 405-411.

[20] Dutta, Prashanta, and Sandip Dutta. "Effect of baffle size, perforation, and orientation on internal heat transfer enhancement." International Journal of Heat and Mass Transfer 41, no. 19 (1998): 3005-3013.

[21] Yang, Yue-Tzu, and Chih-Zong Hwang. "Calculation of turbulent flow and heat transfer in a porous-baffled channel." International Journal of Heat and Mass Transfer 46, no. 5 (2003): 771-780.

[22] Nie, Jian H., Y. T. Chen, and Hsuan-Tsung Hsieh. "Effects of a baffle on separated convection flow adjacent to backward-facing step." International Journal of Thermal Sciences 48, no. 3 (2009): 618-625.

[23] Abu-Nada, Eiyad. "Application of nanofluids for heat transfer enhancement of separated flows encountered in a backward facing step." International Journal of Heat and Fluid Flow 29, no. 1 (2008): 242-249.

[24] Che Sidik, N. A. and Safdari, A. " Modelling of Convective Heat Transfer of Nanofluid in Inversed L-Shaped Cavities." Journal of Advanced Research in Fluid Mechanics and Thermal Sciences 21, no. 1 (2016): 1-12.

[25] Anderson, John David, and J. Wendt. Computational fluid dynamics. Vol. 206. New York: McGraw-Hill, 1995.

[26] Patankar, Suhas. Numerical heat transfer and fluid flow. CRC press, 1980.

[27] Jamil M. M., Che Sidik, N. A. and Muhammad Yazid, M. N. A. W. "Thermal Performance of Thermosyphon Evacuated Tube Solar Collector using TiO2/Water Nanofluid." Journal of Advanced Research in Fluid Mechanics and Thermal Sciences 20, no. 1 (2016): 12-29.

[28] Nor Azwadi, C. S. and Adamu, "Turbulent Force Convective Heat Transfer of Hybrid Nano Fluid in a Circular Channel with Constant Heat Flux." Journal of Advanced Research in Fluid Mechanics and Thermal Sciences 19, no. 1 (2016): 1-9.

[29] Ny, G. Y., Barom, N. H., Noraziman S. M. and S. T. Yeow, "Numerical Study on Turbulent-Forced Convective Heat Transfer of Ag/Heg Water Nanofluid in Pipe." Journal of Advanced Research in Materials Science 22, no. 1 (2016): 11-27.